Fabrication of a segmented micro Penning trap and numerical investigations of versatile ion positioning protocols

M. Hellwig[(a)], **A. Bautista-Salvador**[(a)], **K. Singer**[(a)], **G. Werth**[(b)], **F. Schmidt-Kaler**[(a)]

(a) Institut für Quanteninformationsverarbeitung, Universität Ulm, Albert-Einstein-Allee 11, D-89069 Ulm, Germany,
(b) Physikalisches Institut, Johannes-Gutenberg-Universität, 55099 Mainz, Germany

E-mail: ferdinand.schmidt-kaler@uni-ulm.de

Abstract.

We describe a versatile planar Penning trap structure, which allows to dynamically modify the trapping configuration almost arbitrarily. The trap consists of 37 hexagonal electrodes, each of 300 μm diameter, fabricated in a gold-on-sapphire lithographic technique. Every hexagon can be addressed individually, thus shaping the electric potential. The fabrication of such a device with clean room methods is demonstrated. We illustrate the variability of the device by a detailed numerical simulation of a lateral and a vertical transport and we simulate trapping in racetrack and artificial-crystal configurations. The trap may be used for ions or electrons, as a versatile container for quantum optics and quantum information experiments.

PACS numbers: 37.10.Ty, 03.67.Lx

1. Introduction

Trapped ions have been an important workhorse for quantum information research, even though research has been mostly limited to one dimensional arrangements of ion crystals in radio frequency Paul traps [1, 2]. Planar Paul traps have shown their advantages for scalable micro fabricated devices [3, 4, 5, 6, 7, 8], even for trapping cold molecules [9]. However a two-dimensional arrangement of ions [10] still needs to be shown. Inspired by experiments with large, rotating planar ion crystals in Penning traps [11], as well as single ions [12] or electrons [13, 14], novel designs for Penning traps have been proposed [15, 16]. As an advantage [17], Penning traps operate with only static electric and magnetic fields, thus noise and heating issues as observed for radio frequency ion traps [18] are expected to be largely suppressed. The static magnetic field lifts the degeneracy of ground state spin states, allowing for a natural choice of qubit basis states. Currently, the most urgent unsolved scientific task concerns building a scalable quantum information processing device. In this letter we show that novel planar and micro structured Penning traps allow for trapping various qubit configurations including two-dimensional ion crystals with well controlled interactions between individual qubits and with individual initialization and readout. Cluster state generation and quantum simulation are future applications of such tailored qubit arrays.

The paper first describes a pixel micro structure to generate the complex electric potential for the novel Penning trap. We briefly sketch the numerical method to calculate the potential landscape with the required high accuracy, and optimize the control voltages for a selected set of qubit configurations and qubit operations. We estimate two-qubit spin-spin interactions [19, 20], which would lead either to a multi-qubit cluster state [21] or the realization of plaquette physics [22] in a rich, however well controlled quantum optical few-spin-system. In a last section we show the fabrication of such a device with state to the art clean room technology.

2. Versatile trapping configurations and numerical simulations

Charged particles in Penning traps are harmonically trapped and exhibit three oscillation frequencies: The fastest one, the cyclotron oscillation is perpendicular to the applied strong magnetic field. It amounts to $\omega_{cycl}/(2\pi) = qB/m \sim 400$ kHz/T in case of $^{40}Ca^{+}$ ions and in typical experimental settings with singly charged ions [11, 12] one may reach a few MHz of cyclotron frequency. In the case of trapped electrons [13, 14, 23] the cyclotron frequency easily exceeds even 100 GHz. Confinement along the direction of the magnetic field-lines is assured by an electric field, which in our case is generated by surface electrodes, see Fig. 1. In this confinement the ion oscillates with the axial frequency $\omega_{ax}/(2\pi)$, determined from the electric potential applied to the different pixel electrodes. The ion is trapped in the minimum of the potential $\phi_{el}(z)$ along the z-axis, above the surface. The Penning trap stability condition $2\omega_{ax}^2 < \omega_{cyc}^2$ limits the maximum axial confinement. Additionally, a slow magnetron motion appears

due to an $\vec{E} \times \vec{B}$ drift with a frequency typically much lower than ω_{ax}. Unlike the axial and radial oscillation, the magnetron motion in the xy-plane centers around the maximum of the potential $\phi_{el}(x, y)$, a peculiar feature of Penning traps. In a complex geometry such as our Pixel trap with a large number of different electrodes to control the confinement, see Fig. 1a, numerical simulations are used to find a set of voltages for specific tasks and configurations with a few ion qubits.

For the shape of the control electrodes, we decided to use a hexagonal shape with a diameter (tip to tip) of 300μm, which allows the forming of spherically symmetric potential field geometries.

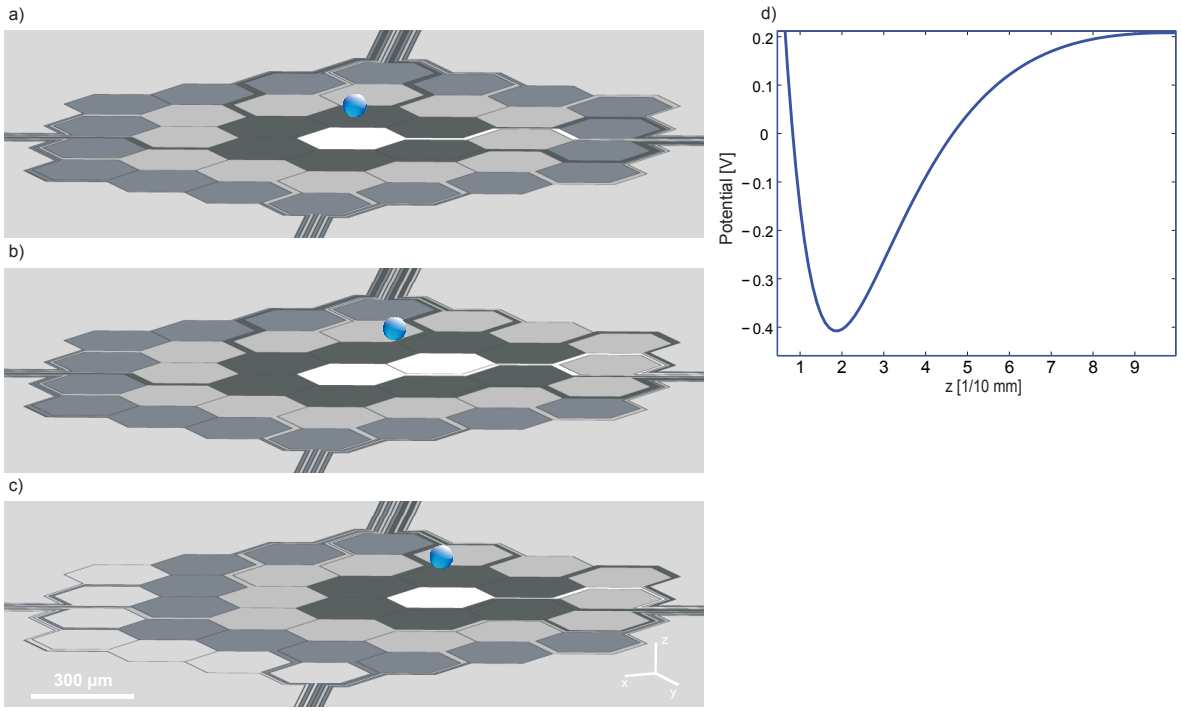

Figure 1: a) Schematics of the pixel trap for single ion trapping and b, c) for a lateral transport of an ion by changing of applied potentials. d) Potential $\phi_{el}(z)$ relevant for the axial confinement. If we chose addressing the pixels with 1 V: white, -2.8 V: black, 1 V: light grey, and 3 V: dark grey, we result in an axial frequency of $\omega_{ax}/(2\pi) = 1.6$ MHz for calcium-ions. The magnetic field points out of orthogonal to the plane of electrodes.

In order to obtain accurate noise free electrostatic potentials for our geometry we apply the fast multipole method for the boundary element problem[36]. Therefore a mesh of $N \sim 12446$ surface rectangles is placed on the surface geometry and the surface charges are then obtained in only $O(N)$ steps. As opposed to finite elements or difference methods only surface elements have to be meshed. When the surface charges for the individual voltage configurations are calculated the potential at any point in space can be obtained by summing over the surface charges weighted by a distance dependent $1/r$ scaling function.

2.1. Single ion trapping

For an initial trapping of ions, one usually chooses a large trapping volume. To that end all control voltages of the pixels are set to 0 V while the outer four circular segments are at -10 V and the outermost bits at +10 V. The resulting potential exhibits an axial frequency of 500 kHz and a depth of 3.5 eV, ideally suited for trapping, cooling and observing a large cloud, see Fig. 2.

Starting from this initial setting, the inner electrodes are employed for single ion trapping and we make use of the advanced configurations possible in a pixel-trap. Optimal potentials are obtained by applying regularization techniques [36]. If we supply the voltages 0 V (white), -0.2369 V (black), 1.3171 V (light grey), -28.3125 V (dark grey), 8.1845 V (quartered ring, black), 10.2997 V (outside plane, grey), see figures 1a) and 2a), we would be able to reach a tight trap with an axial frequencies of ~ 1 MHz and a trap-depth of ~ 0.7 eV. The trap minimum is located at a distance of ~ 0.2 mm from the electrode surface, the anharmonicities are minimal and only lead to a broadening of the trap frequency well below a kHz for a particle as hot as 5 K. We propose to load and laser-cool ions in the deep potential (see previous paragraph) and then alter the voltages to generate a harmonic well.

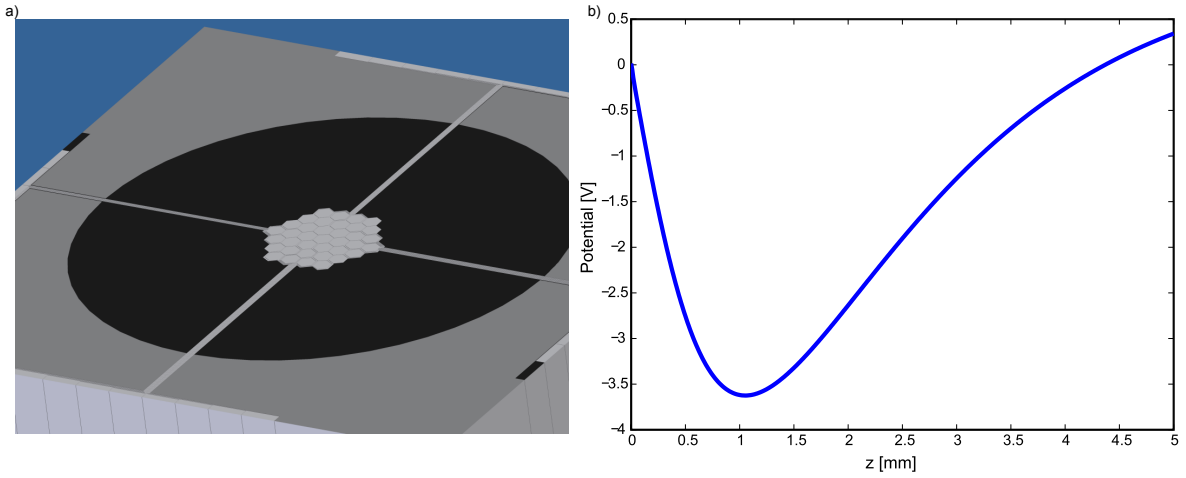

Figure 2: a) Configuration with a large trapping volume and a deep confining potential. All the hexagons are set to 0 V, the quartered ring around it serves as the first ring electrode at -10 V and the rest serves as the outer ring electrode with 10 V. b) Axial trapping potential.

2.1.1. Transporting a single ion Ions may be transported in the pixel trap either (i) orthogonal to the plane of electrodes, a transversal transport, or (ii) in a lateral transport parallel to the trap electrode surface. In the case of (i) the pixels are arranged as rings on equal potential, such that the position of the minimum of the axial potential varies [24]. A possible application of a transversal transport would be the determination of

motional heating and decoherence rates as a function of ion-surface distance, similar to attempts for dynamic Paul traps [25]. The lateral transport is sketched in Fig. 1 (a) to (c) (conceptually) as well as Fig. 3 (radial potentials). Starting out with a configuration that uses a single pixel as its center, we widen it up to an elongated center, including adjacent pixels, then we tilt the potential in the direction of the new center and finally finish with a single ion confinement at the displaced position. The ion is confined near the *maximum* of the radial electric potential $\Phi_{rad}(x, y)$ as the magnetron oscillation corresponds to an inverted harmonic potential. Axialisation, an excitation of the ion's magnetron frequency, centers it to Φ_{rad}^{max}. Experimentally, the outer four segments, see Fig. 2 may be employed to generate a rotating wall potential for this excitation.

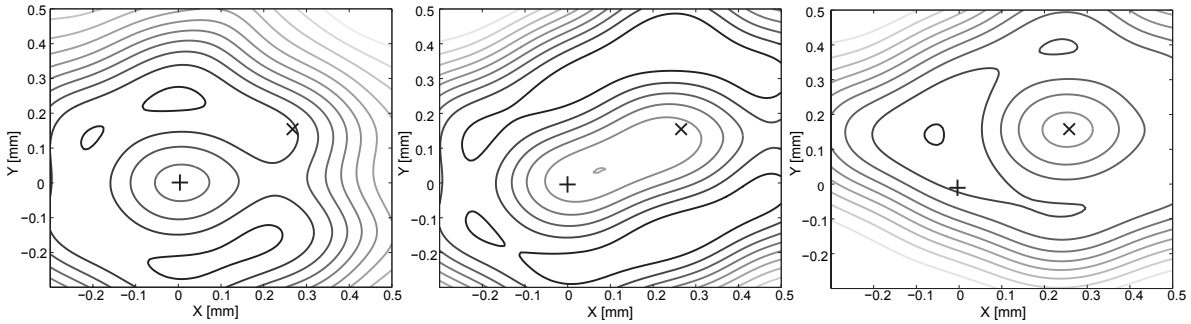

Figure 3: $\Phi_{el}(x, y)$ of the electrode-configuration used at the start, in the middle and at the end of the transport, respectively, shown as a contour-plots. The starting-position of the transport is marked with $\bigoplus$, the end-point with $\bigotimes$.

The lateral transport of single ions may be readily expanded to a joining and splitting operation for two ion crystals, a technique which has been so far limited to segmented linear Paul traps [29, 30, 31].

2.2. Ring crystals and racetrack configuration

In a linear Paul trap, typically ions arrange as linear ion strings, while two- or three-dimensional arrangements of ions [26] suffer from micro motion in the dynamical trapping field. Here, a clear advantage of the purely static electric field of a Penning trap becomes evident. Two-dimensional "artificial ion crystals" may be trapped by creating multiple trapping sites. We highlight this with an arrangement of sites around a circle, trapping for example three ions in predefined places. One example of such electrode-configuration is shown in figure 4a. The potential in the xy-plane above such an electrode-configuration is displayed in figure 4b with three trapping sites. The interest of the Pixel Penning trap is that various different kinds of such configurations may be converted into each other by a time-dependent addressing of the pixel electrodes.

The colloquial term "racetrack" is commonly used for a configuration in which the trapping-zone is in the form of a ring. Radio frequency ion traps have been used

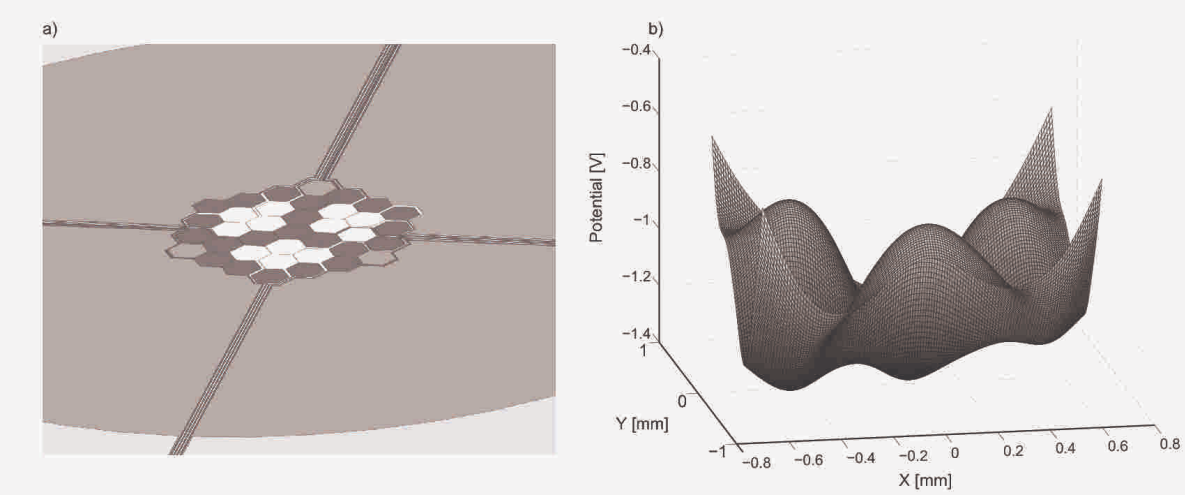

Figure 4: a) Electrode-configuration for an artificial ion crystal with three sites. With voltages of 0.6 V: white, -4.0 V: dark grey, 0.5 V: light grey, we reach a trap depth of 0.8 eV and axial frequencies near 800 kHz. b) xy-potential of the trapping configuration shown in figure 4a), an artifical ion crystal with three ions.

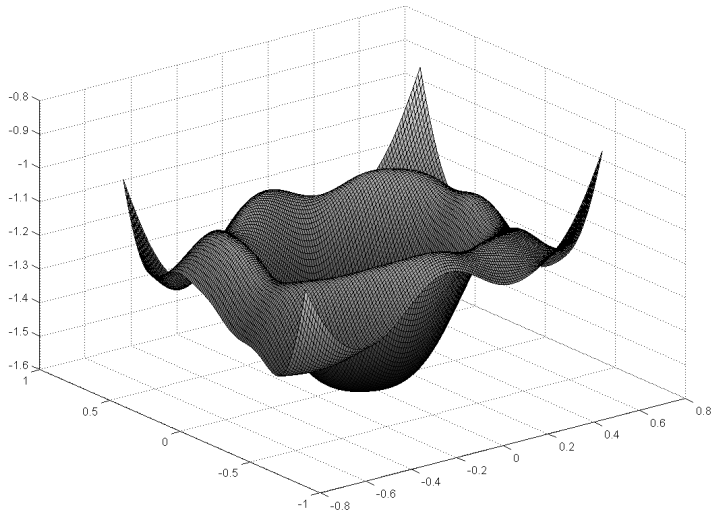

Figure 5: Resulting potential $\Phi_{el}(x, y)$ for a racetrack configuration. Voltages are: on the track: 1, 1.5, 0.8, 2, 0.8, 1, 0.6, 1.3, 1, 2, 1 and 2 V in a righthand circle (due to slightly varying sizes of the hexagons). The ring directly inwards of the track is at -4 V, the point in the middle at -0.8 V, the ring directly outwards at -4.8 V and the outermost parts of the track at +0.2 V.

to hold linear crystals in a racetrack configuration [27], inspired by confined charged particles in accelerator rings. Magnetic traps with additional radio-frequency fields have

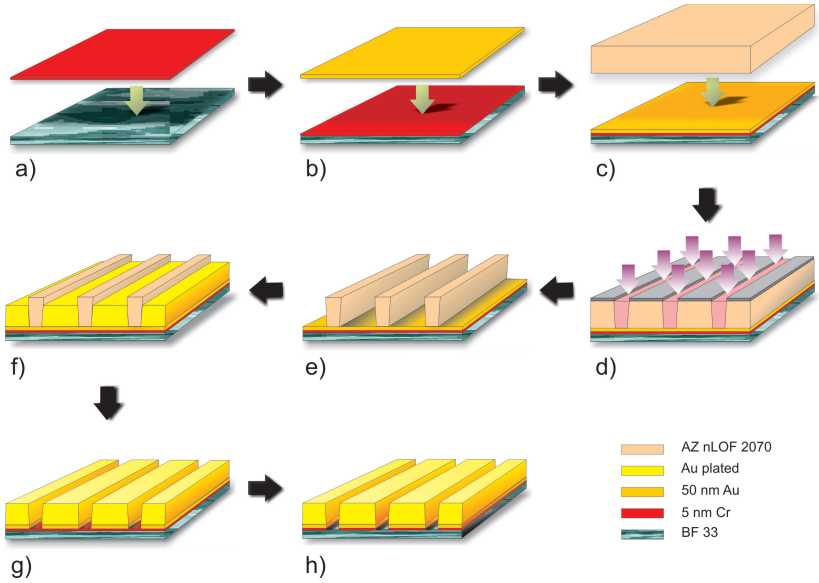

Figure 6: Simplified scheme of the fabrication process. a) Evaporation of the adhesion Cr layer on BF® 33 wafer, b) Evaporation of the starting Au layer on Cr/BF® 33, c) Spin coating of AZ nLOF 2070 resist, d) Photolitography: exposure to UV light, e) Development, f) Electroplating of Au, g) Stripping of resist and wet-etching of Au seed layer, h) Wet-etching of Cr.

been proposed for racetrack configurations for interferometric purposes [28]. Optical potentials for trapping neutral atoms [32, 33] are yet another option. Our Penning trap approach does not require any time dependent fields, advantageous with regard to heating and decoherence, and technically less demanding. In the Pixel Penning trap we may realize a 580 μm diameter racetrack, see Fig. 5.

3. Fabrication of the Pixel trap

Starting with the CAD file of the trap design, we realize the fabrication of planar Penning traps by three-step clean room processing: photolithography, electroplating and etching. The fabrication is schematically presented in Fig. 6. A polished borosilicate glass wafer serves as substrate. We have achieved similar results with 2" sapphire wafers of thickness 0.50 mm, which has the advantage of better heat conduction, even at cryogenic temperatures. In order to ensure proper adhesion of the Au electrodes to the substrate an adhesion promoter layer is mandatory. We use a 5 nm Cr layer deposited on the wafer via thermal evaporation. Furthermore, to enhance Au electrodeposition a 50 nm Au seed layer is also thermally deposited on top and a negative resist ‡ is added. Photolithography is then carried out. The mask resist lines which define the gaps between electrodes show a width of 4.0 μm. Electrodes are grown up to 4.0 μm in

‡ AZ® nLOF 2070

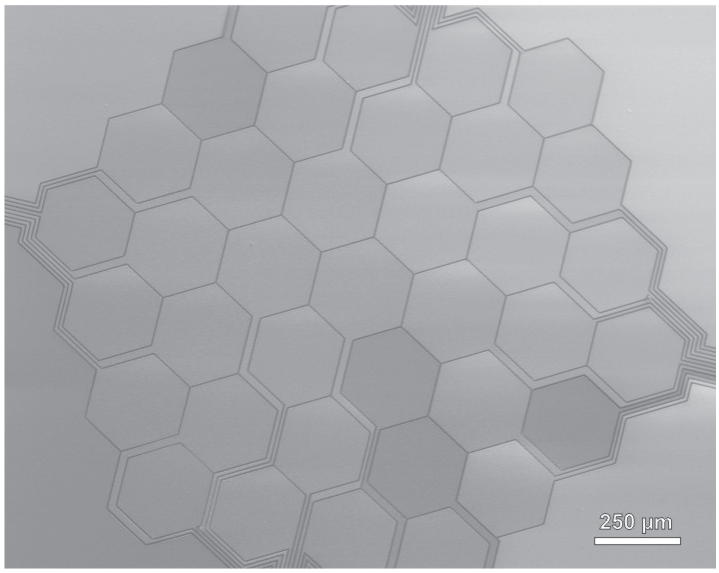

Figure 7: SEM micrograph of the Gold-on-sapphire Pixel Penning trap

.

a Au plating bath §. We achieve an aspect ratio of 1, shielding inter-electrode insulating substrate gaps from the ion position. After electroplating the resist mask is stripped off. The Au seed layer is removed and a final Cr etching step is performed. Fig. 7 shows an Scanning Electron Microscopy micrograph of the inner center of the Pixel trap.

We dice the wafers and ball bond the chip electrodes to an 84-pin Kyocera chip carrier using 25 μm Au wires. Under UHV conditions with 10^{-7} mbar we investigate the limit of the applied electric field by raising slowly the applied voltage. We observe a breakdown at approximately 180 V for 1.2 μm to 720 V for 4.0 μm gap-width, respectively, far above the required trap voltages.

4. Outlook

As a next step, we plan experimental tests with single trapped $^{40}Ca^{+}$ ions in the pixel trap in order to particularly optimize the control of the transport processes [34, 35]. The pixel trap opens a way to miniaturized Penning traps, and once the coherence properties have been tested with single ions close to surfaces, one might further reduce the spatial dimensions of the surface electrodes to about 10 μm, including a dual layer technique [8]. With ion-ion distances in the 10μm range, entanglement gate operations mediated by an additional inhomogenious magnetic field [19] reach a coupling strength of a few kHz for the mutual effective spin-spin coupling under realistic experimental conditions. State transfer protocols, quantum simulation, and a generation of cluster states using two-dimensional ion crystals would be further perspectives.

§ mixture of Enthone GRC complex and Enthone microfab Au-100B

Acknowledgements

A. B.-S. thanks CONACYT for financial support through the scholarship ID 206267. We acknowledge financial support by the German science foundation DFG within the SFB/TRR-21, the European commission within MICROTRAP (Contract No. 517675) and the excellence program of the Landesstiftung Baden-Württemberg.

References

[1] H. Häffner, C. F. Roos, R. Blatt, Physics Reports 469, 155 (2008).
[2] R. Blatt and D. J. Wineland, Nature 453, 1008 (2008).
[3] M. J. Madsen, W.K. Hensinger, D. Stick, J.A. Rabchuk, and C. Monroe, Appl. Phys. B 78, 639 (2004).
[4] C. E. Pearson, D. Leibrandt, W. S. Bakr, W. J. Mallard, K. R. Brown, and I. L. Chuang, Phys. Rev. A 73, 32307 (2006).
[5] S. Seidelin, et. al., Phys. Rev. Lett. 96, 253003 (2006).
[6] D. Leibrandt, R. J. Clark, J. Labaziewicz, P. Antohi, W. S. Bakr, K. R. Brown, and I. L. Chuang, Phys. Rev. A 76, 55403 (2007).
[7] S. Wang, J. Labaziewicz, Y. Ge, R. Shewmon, and I. L. Chuang, App. Phys. Lett. 94, 094103 (2009).
[8] J. M. Amini, J. Britton, D. Leibfried, and D. J. Wineland, arXiv:0812.3907
[9] M. Debatin, M. Krner, J. Mikosch, S. Trippel, N. Morrison, M. Reetz-Lamour, P. Woias, R. Wester, M. Weidemüller, Phys. Rev. A 77, 033422 (2008).
[10] R. Schmied, J. H. Wesenberg, D. Leibfried, Phys. Rev. Lett. 102, 233002 (2009).
[11] F. Skiff and J. Bollinger, M. J. Jensen, T. Hasegawa, and J. J. Bollinger, Phys. Rev. A 70, 033401 (2004).
[12] D. R. Crick, H. Ohadi, I. Bhatti, R. C. Thompson, and D. M. Segal, Opt. Express 16, 2351 (2008).
[13] L. S. Brown and G. Gabrielse, Rev. Mod. Phys. 58, 233 (1986).
[14] D. Hanneke, S. Fogwell, and G. Gabrielse, Phys. Rev. Lett. 100, 120801 (2008).
[15] J. R. Castrejón-Pita and R. C. Thompson, Phys. Rev. A, 71, 1 (2005).
[16] J.R. Castrejón-Pita, H. Ohadi, D.R. Crick, D.F.A. Winters, D.M. Segal and R.C. Thompson, J. Mod. Opt 54, 1581 (2007).
[17] J. M. Taylor, T. Calarco, arXiv:0706.1951
[18] J. Labaziewicz, Y. Ge, P. Antohi, D. Leibrandt, K. R. Brown, and I. L. Chuang, Phys. Rev. Lett. 100, 13001 (2008).
[19] M. Johanning, A. Braun, N. Timoney, V. Elman, W. Neuhauser, Chr. Wunderlich, Phys. Rev. Lett. 102, 073004 (2009).
[20] N. Daniilidis, T. Lee, R. Clark, S. Narayanan, H. Häffner, J. Phys. B 42, 154012 (2009).
[21] H. Wunderlich, Chr. Wunderlich, K. Singer, F. Schmidt-Kaler, Phys. Rev. A 79, 052324 (2009)
[22] B. Paredes and I. Bloch, Phys. Rev. A 77, 023603 (2008).
[23] P. Bushev, S. Stahl, R. Natali, G. Marx, E. Stachowska, G. Werth, M. Hellwig and F. Schmidt-Kaler, Euro. Phys. Journal D, 50, 97 (2008).
[24] I. Marzoli, et. al., J. Phys. B: At. Mol. Opt. Phys. 42, 154010 (2009).
[25] L. Deslauriers, S. Olmschenk, D. Stick, W. K. Hensinger, J. Sterk, C. Monroe, Phys. Rev. Lett. 97, 103007 (2006).
[26] P.F. Herskind, A. Dantan, M.Albert, J.P. Marler, M. Drewsen, Journal of Physics B: Atomic, Molecular and Optical Physics. Vol. 42(15), 154008 (2009).
[27] G. Birkl, S. Kassner, H. Walther, Nature 357, 310 (1992).
[28] I. Lesanovsky, W. von Klitzing, Phys. Rev. Lett. 99, 083001 (2007).
[29] M. A. Rowe et. al., Quantum Information and Computation 2, 257 (2002).

[30] G. Huber, T. Deuschle, W. Schnitzler, R. Reichle, K. Singer, F. Schmidt-Kaler, New J. Phys. 10 013004 (2008)
[31] R. B. Blakestad, C. Ospelkaus, A. P. VanDevender, J. M. Amini, J. Britton, D. Leibfried, and D. J. Wineland, Phys. Rev. Lett. 102, 153002 (2009).
[32] A. Kaplan, N. Friedman, M. Andersen, N. Davidson, Phys. Rev. Lett. 87, 274101 (2001)
[33] C. Ryu, M. F. Andersen, P. Clad, Vasant Natarajan, K. Helmerson, and W. D. Phillips Phys. Rev. Lett. 99 260401 (2007).
[34] D. Kirk, Optimal Control Theory An Introduction (Dover Publications, Mineda, NewYork, 2004).
[35] G. De Chiara, T. Calarco, M. Anderlini, S. Montangero, P. J. Lee, L. Brown,W. D. Phillips, J. V. Porto, Phys. Rev. A, 77, 052333 (2008).
[36] K. Singer, U. Poschinger, M. Murphy, P. Ivanov, F. Ziesel, T. Calarco, and F. Schmidt-Kaler, "Colloqium: Experiments with atomic quantum bits - essential numerical tools", arXiv:0912.0196 (2009).